Pattern Recognition Pergamon Press 1973. Vol. 5, pp. 175–197. Printed in Great Britain

The "Rubber-Mask" Technique—I. Pattern Measurement and Analysis

BERNARD WIDROW

Department of Electrical Engineering, Stanford Electronics Laboratories, Stanford, California 94305, U.S.A.

(*Received* 18 *December* 1972 *and in revised form* 10 *April* 1973)

Abstract—Template matching is a fundamental technique of pattern recognition. Although this technique is very general, its applicability has been limited because of the difficulty often encountered when fitting templates to natural data. Natural patterns are often distorted, misshapen, stretched in size, fuzzy, rotated, translated, observed at an unusual perspective, etc. Flexible templates (rubber masks) have been devised which, when fitted to natural data, can be used for measurement, data reduction, data smoothing, and classification of highly irregular waveforms and image shapes. These problems had been largely unsolved by existing template matching methods.

Specific applications to the analysis of human chromosome images, chromatographic recordings, electrocardiogram waveforms, and electroencephalogram waveforms are illustrated. The rubber-mask technique will probably be usable in a wide variety of scientific applications.

Flexible templates Rubber masks Irregular pattern measurement Data reduction Chromosome images Chromatographic waveforms Electrocardiogram waveforms Electroencephalogram waveforms

1. INTRODUCTION

MUCH work has been done during the past twenty years in the field of pattern recognition, both theoretical and practical. Several of the schemes that have evolved with matched filters, linear threshold classifiers, and nearest neighbor rules are optimal in some sense;[1–5] but most are *ad hoc* and have been developed to solve specific problems. On the practical side, the work in optical character recognition has been the most successful.[6–8]

It is hard to typify work in the field because of the profusion of pattern-recognition schemes. However, it is possible to divide the field into two broad schools: one that classifies by comparing *feature observations* with pattern property lists; and another that uses the pattern information directly and classifies by means of some form of *template* matching. Other schools may mix these approaches, but the two basic approaches remain.

Pattern features are often found to be invariant to translation, rotation, scale, etc. It is desirable to select such features as a basis for classification. However, there is no general method for choosing or designating features. A feature-detection system, unless very specially tailored to the particular problem, could miss important attributes. Nevertheless, feature detection will retain a permanent place in the methodology of pattern recognition.

The emphasis of this paper will be on template matching. The advantage of template matching comes from being able to use patterns directly without the need for devising, detecting, or measuring special features. The pattern image itself contains all the required information. We are concerned, however, with pattern matching in the presence of rotation, translation, scale change, differing shadow and lighting effects, gross shape distortion, and

random noise which makes the pattern fuzzy. Because of the recurrence of such distortions in most data patterns, template matching generally does not work very well.

It is the purpose of this paper to show how template matching can in many cases be used in pattern measurement and analysis, even when patterns are highly irregular in shape. Computer-implemented or computer-simulated flexible templates are proposed. We call these "rubber masks".

The human eye can determine that two non-exactly-matching signatures were made by the same hand. The eye/brain can determine that a face being viewed has been seen before, only not with the same perspective or with the same light and shadows. The eye/brain is remarkably able to ignore pattern variations that for the most part should be ignored. The ability of the eye/brain system to match patterns in the presence of distortion would be useful for incorporation into practical automatic pattern-recognition systems. It is possible that such an ability may be realized in a general way through the use of the flexible masking techniques to be described in this paper.

The flexible template, the rubber mask, is in effect an unusual form of adaptive multi-dimensional matched filter. The basic template could be formed from a mathematical pattern model or from natural pattern data. Rubber masks have been parameterized and adapted as illustrated here with a series of applications to the analysis of chromosomal images, liquid and gas chromatograph output records, electroencephalogram (EEG) waveforms, and electrocardiogram (EKG) waveforms.

2. CHROMOSOME ANALYSIS AND CLASSIFICATION

Chromosome patterns are generally observed under a light microscope that magnifies image size about 2000 times. The chromosomes of a single human cell vary considerably in size. The length of the smallest corresponds to only about ten wavelengths of light in the center of the visible band. Consequently, microscopic images of chromosomes are generally fuzzy, pushing the ultimate resolving limits of light microscopy.

Human chromosome preparations are often made from blood cells or from cells grown in culture. A hypotonic solution is used to swell the cells which are then fixed in acetic alcohol. Cells suspended in the fixative are then dropped from a height onto a glass microscope slide in order to spread the chromosomes. At this point, various stains may be chosen and applied to the cells. Cells caught at "metaphase," i.e. when they are dividing, exhibit their chromosome complement separated in a "spread." Only a small fraction of the cells are at metaphase at a given time. Thus one observes on a glass slide a few stained chromosome spreads amid a sea of stained non-dividing cells. A human chromosome spread (in this case an abnormal one with extra chromosomes) is pictured in Fig. 1.

At metaphase each chromosome has a twin, normally an identical counterpart. The cytogeneticist first associates the pairs, then karyotypes the chromosomes, i.e. classifies them into groups and orders the individuals within the groups. This is a time-consuming and not always error-free process. The problem is difficult, not only because the patterns are fuzzy, but also because the chromosomes sometimes touch one another, or even overlap one another. Furthermore, the "arms" of the chromosomes are often twisted and misshapen due to impact resulting from the samples being dropped onto the glass slide during chromosome preparation.

Chromosomes are karyotyped by their arm lengths and by their shapes. Existing automatic recognition techniques have classified chromosomes on the basis of measurements

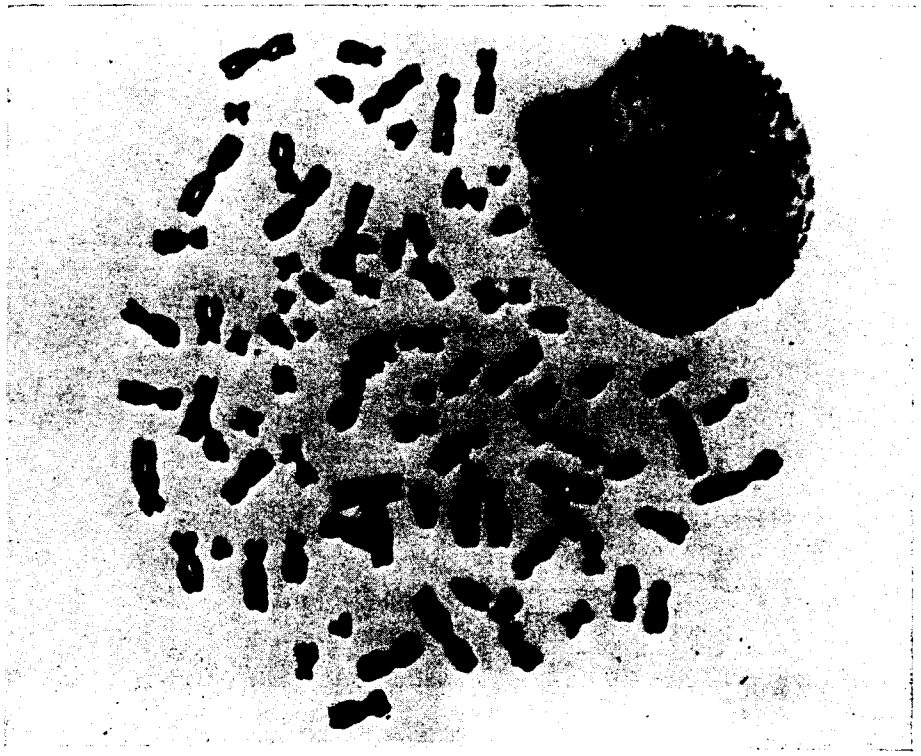

FIG. 1. A human chromosome metaphase spread.

[*facing* p. 176]

FIG. 8. Liquid chromatograph in the laboratory.

such as centromeric index (ratio of arm lengths to total body length), ratios of body lengths from one chromosome to another, chromosome areas, etc. Unfortunately, these parameters cannot generally be measured accurately. It is possible to measure the length of a table top quite accurately and consistently, but it is not easy to measure the length of a chromosome arm which may be twisted and fuzzy. Thus it is almost impossible to determine where the arm begins and where it ends (see Fig. 1).

The rubber mask technique is being developed for the purpose of accurately measuring chromosome geometrical properties. Computer implementation is essential, requiring digitized input patterns. Examples of digitized chromosome images are presented in Fig. 2. Two levels of gray scale were established by reference to an adjustable black/white intensity threshold. Altering the threshold level would have some effect on this form of pattern; it might even be desirable to take several digitizations of the original image with different threshold settings. In any event, the sample patterns in Fig. 2 are typical of those that have been subjected to analysis by rubber masking.

The rubber-mask technique is applied by comparing the shapes of digitized data-sample patterns with those of stored standard patterns. The stored stereotype (idealized pattern) is progressively distorted until the data pattern is fitted to the desired degree of accuracy. The successive distortions, or iterations, to which the stereotype is subjected constitute, in effect, the evolution of a stretched template (rubber mask). By means of a system of coordinates and parameters, the shape finally assumed by the rubber mask can be numerically described.

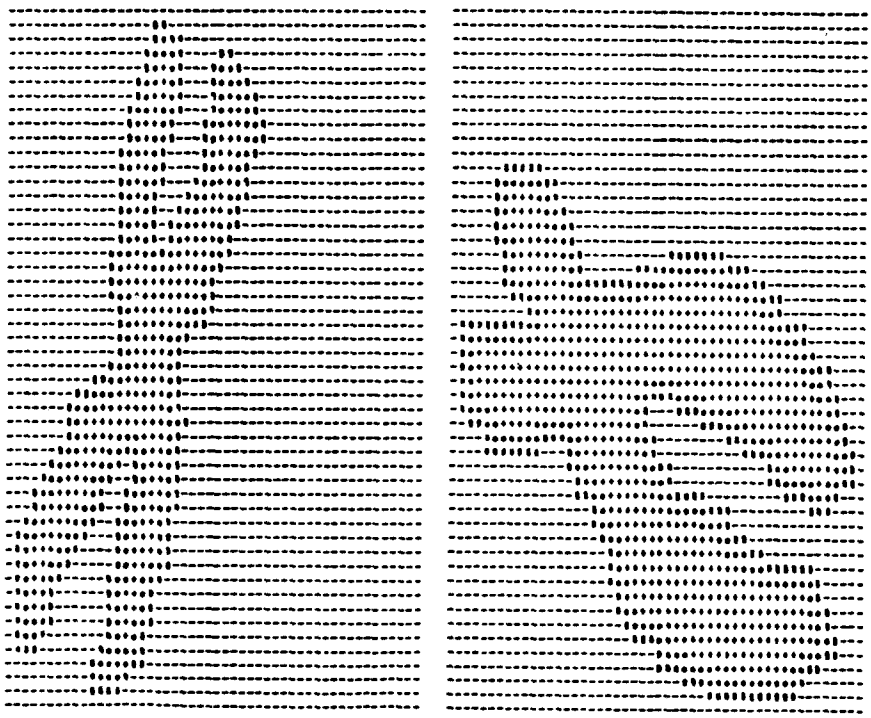

FIG. 2. Two-level digitization of chromosome images.

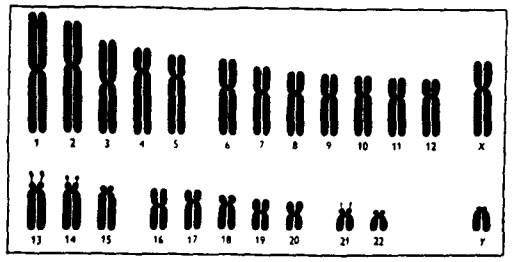

(a) "DENVER STANDARDS"

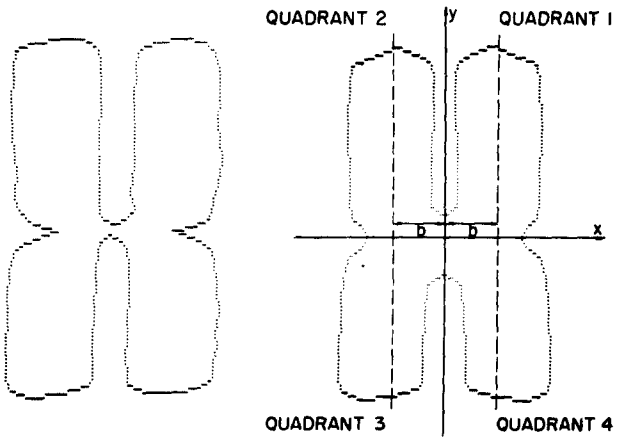

(b) A DIGITIZED "DENVER STANDARD"

(c) MODIFIED "DENVER STANDARD"

FIG. 3. Human chromosome stereotypes.

A rubber-mask chromosome analysis has been made using various versions of the "Denver Standard" chromosomes as stereotypes. These are shown in Fig. 3a. These standard shapes, arranged in a karyotype, were established at a meeting of cytogeneticists organized by T. T. PUCK in Denver in 1960.[9] They were designed to be chromosome-like in shape and to have ratios of upper arm length to lower arm length and arm length to total length which are average for normal human chromosomes. One of these standards (No. 3) was chosen as a stereotype for the present study (illustrated in Figs. 4 and 7) and is shown magnified and in digitized form in Fig. 3b. The form was modified somewhat by adding girth at the center (centromere) in order to create a shape somewhat closer to that of an actual human chromosome. The modified standard chromosome is shown in Fig. 3c. Note the addition of a coordinate system and of dotted lines which are median lines through the chromosome arms. These are essential in keeping track of the distortion process necessary to fit the template to the data sample.

An illustration of template fitting is shown in Fig. 4. The stereotype (the modified Denver Standard No. 3) is shown in Fig. 4a. The digitized sample of a human chromosome to be fitted is shown in Fig. 4e. Distorted versions of the stereotype at different iterative

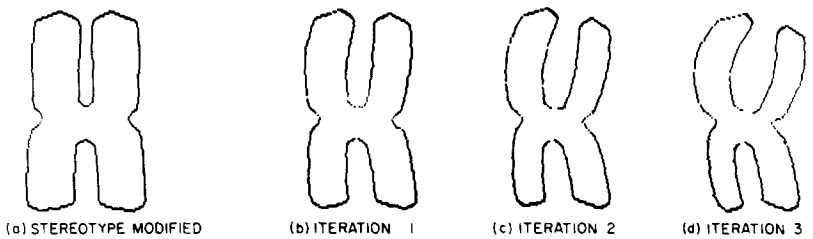

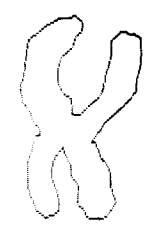

QUADRANT	1	2	3	4	1	2	3	4	1	2	3	4
LENGTH	-3	0	-3	-4	-6	0	-5	-8	-9	0	-7	-12
WIDTH	-1.5	8	-4	6	-3.2	17	-8	13	-5	25	-12	19
ANGLE	40	-50	-3	25	80	-100	-7	50	120	-150	-10	75
CURVE	-27	53	20	-7	-54	106	40	-14	-80	160	60	-20

(f) ANGLE, CURVE, WIDTH AND LENGTH FOR EACH ITERATION

FIG. 4. Stretching a chromosome stereotype to fit natural data.

stages are shown in Figs. 4b–d. Corresponding sets of distortion parameters are listed in Fig. 4f. Through succeeding iterations, the distorted stereotype (stretched template) is seen to experience an evolution of its shape toward that of the chromosome to be fitted.

An explanation of the distortion parameters that have been used in this study, namely LENGTH, WIDTH, ANGLE, and CURVE, is presented in Fig. 5. These parameters are adjusted individually and independently in each of the four quadrants of the stereotype as defined in Fig. 3c. Each arm can be lengthened or shortened, thickened or thinned, offset at an angle along its median line, or curved with a second degree function along its median line; or it can be distorted with a combination of these effects.

LENGTH $$y' = y + y \cdot \frac{\text{LENGTH}}{100}$$, where LENGTH = % increase in length

WIDTH $$x' = x + (x - b) \cdot \frac{\text{WIDTH}}{100}$$, where WIDTH = % increase in width

ANGLE $$x' = x + y \cdot \text{ANGLE} \cdot k_1$$

where k_1 is a constant chosen so that an ANGLE value of 100 will bend the arm so that the distance from its tip to the y-axis is doubled.

CURVE $$x' = x + y^2 \cdot \text{CURVE} \cdot k_2$$

where k_2 is a constant chosen so that a CURVE value of 100 will bend the arm so that the distance from its tip to the y-axis is doubled.

FIG. 5. Chromosome distortion parameters.

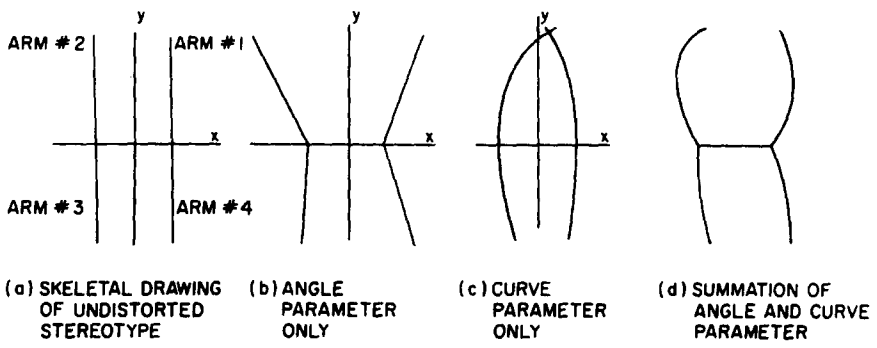

FIG. 6. Skeletal illustration of chromosome distortion parameters.

The distortion undergone by the stereotype is indicated in skeletal form in Fig. 6. The undistorted stereotype is represented by the "H-pattern" in Fig. 6a. The vertical lines are the median lines through the stereotype arms (refer to Fig. 3c). Figure 6b illustrates the effect of ANGLE only applied to the median lines, while Fig. 6c shows the effect of CURVE only. Figure 6d is a skeletal view of the distorted stereotype incorporating the summed effects of ANGLE and CURVE. Although the effects of LENGTH and WIDTH are not included in this figure, the general shape of the distorted stereotype is quite evident.

A blow-up of the distorted stereotype superposed upon a blow-up of the sample pattern of a human chromosome is shown in Fig. 7. This figure illustrates many aspects of the rubber-mask idea. The "rubberized" template (distorted stereotype) is equivalent to a smoothed version of the actual data, the digitized human chromosome. The "fit" is optimized with the aid of the computer, which counts the number of units of area in the portions of the patterns which are not congruent. The distorted stereotype (rubber mask) is changed by an iterative process until this error count is minimized.

The fitted stereotype (solid outline) could conceivably be used in many circumstances in place of the actual digitized human chromosome (dotted outline). Such use would comprise a form of *data reduction.* The data image would be represented approximately by the combination of the known undistorted stereotype and by a small number of numerical distortion parameters.

Another application for the fitted stereotype could result in feature measurement. Arm lengths, widths, areas, and centromeric index of the human chromosome could be estimated in terms of the lengths and widths and areas of the distorted stereotype by including the length and width factors derived from the fitting process. (The parameters ANGLE and CURVE are merely used in the fitting process and have no value in measuring and classifying chromosomes.)

By placing narrow limits on the variability of the LENGTH and WIDTH parameters, the chromosomes of the spread (Fig. 1) could be karyotyped by associating each data chromosome with the individual modified Denver Standard chromosome that it best fitted. This would require the use of 24 different stereotypes. A more practical approach might be to select a representative stereotype for each of the chromosome groups, comprising Nos. 1–5, 6–12, 13–20, 21–22, X, and Y. A data chromosome would then be grouped by determining to which representative stereotype it could best be fitted. Its position or

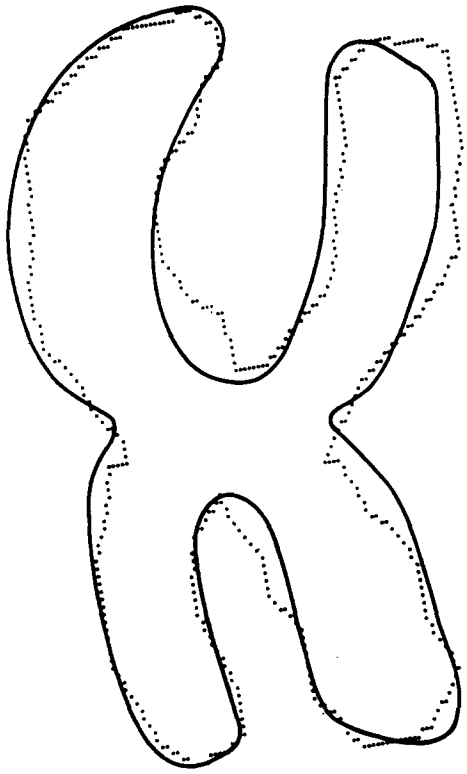

FIG. 7. Rubber mask at iteration #3 (solid) compared with natural chromosome (dotted).

rank within the group would then be determined by the LENGTH and WIDTH parameters.

The template-fitting experiments illustrated here have been done semiautomatically using an interactive computer terminal. The position and orientation of the axes of the rubber mask relative to those of the data chromosome have been chosen and modified by man/machine interaction. The same is true of the four individual parameters in each quadrant. The number of adjustable parameters is sixteen, plus two for X–Y placing of the mask axes, plus one more for axis rotation, giving a total of nineteen adjustables.

A scheme for fully automatic adjustment is currently under development. A method of initially guessing the centromeric position is being tested which finds four points on the data chromosome located where the arms join in indentations. Diagonal lines through these points cross at a point which seems to be a reasonable initial estimate of the centromere position. The initial angular orientation for the rubber mask is determined by rotating the data pattern so that when squeezed in a software-implemented "vise," a minimal "jaw opening" is obtained. The axes of the rubber mask are initially aligned parallel to the simulated vise jaws. The initial centromere is chosen as above. An iterative process then commences to vary all nineteen parameters in search of a best fit.

Gradient methods are being developed to reduce computation time. Preliminary results show that, using the initial conditions of centromere and angle described above, global optima are attained after small numbers of iterative computational cycles.

Recent research into new staining techniques has resulted in chromosome "banding patterns".[10,11] Under suitable preparation of samples, dark and light bands appear across the chromosome arms. These bands can be photographed or viewed under the microscope. The widths, spacings, and numbers of bands are characteristic of the individual chromosomes in the karyotype. Now, difficult-to-resolve chromosomes are easily separated, greatly simplifying the karyotyping problem.

Work is just beginning on the application of the rubber-masking principle to the problem of measuring geometric properties of banding patterns. Stereotypes of human-chromosome banding patterns have appeared in the literature[12] and this is of great assistance to the development of rubber masks for banding patterns. The banding stain preparations are at present in relatively early stages of development and difficulty is encountered with high variability in the banding patterns. However improvements in preparation techniques are continually appearing in the literature and the usefulness of the banding technique in accurate karyotyping and in the detection of chromosomal abnormalities is being demonstrated in the laboratory.

Two-dimensional rubber masks are illustrated in Figs. 4 and 7. Three-dimensional rubber masks for chromosome banding patterns are being developed adding optical density as another dimension. Actual banding patterns have very wide variations in optical density,[13] and fitting to these variations may turn out to be very advantageous.

The goal of this work is to be able to measure automatically a number of useful geometrical and banding-pattern parameters on individual human chromosomes. If this can be done cheaply enough, the process could be applied in making measurements on the chromosomes of hundreds of cells from the same patient sample. Averaging could provide unprecedented accuracy, effectively placing a new research instrument into the hands of the cytogeneticist to study normal and abnormal measurements. Accuracies of the order of a few per cent is the long-term goal.

The work on chromosome measurement and analysis reported in this section is being developed in collaboration with Dr. Leonard Hayflick of the Stanford University Department of Medical Microbiology. His research interest is in reproducibly growing human cells in nutrient solution in sufficient quantity to make them available to workers all over the world who require standardized sample cells for their experiments. Chromosomal measurement is useful for quality control of the experimental tissue.

3. CHROMATOGRAM ANALYSIS

Figure 7 illustrates a technique for measuring highly irregular shapes, i.e. the digitized shapes of human chromosomes. The same principle could be applied in the analysis of *chromatograms* outputted by liquid or gas chromatographic systems.

Liquid chromatography is gaining increased importance in the clinical determination of amino-acid content of biological samples, typically taken from blood serum or urine. Certain forms of physical disorders, birth defects, mental disorders, etc., can be diagnosed or predicted from the analysis of amino-acid chromatograms. These are graphical outputs, generally recorded on a strip chart, exhibiting a series of peaks. Each amino acid corresponds to an individual peak. The amount of amino acid corresponding to a given peak is

proportional to the area under the peak. For analysis of amino acids in blood or urine in clinical application, the chromatograph equipment does not have the resolution to separate all of the peaks for quantitative measurement. Some of the peaks tend to overlap and linearly add in output amplitude. The problem is to find the areas under the individual peaks in spite of overlap and possible baseline drift. Similar problems in peak picking and area analysis also exist for measuring amino acids by gas chromatography. In both chromatographic techniques, it is desirable to locate the individual peaks accurately in time in order to properly identify the associated amino acid.

Figure 8 shows the amino-acid analyzer, a liquid chromatographic instrument that has been the source of data for this research. Dr. Klara Efron, a pediatrician at the Stanford University Medical Center, has worked with an Electrical Engineering Department student team in preparing the chromatograms for analysis using rubber-mask techniques. The analytical results are checked by testing against known mixtures of amino acids that have been prepared by Dr. Efron. Each sample, whether it is from a human patient or whether it is a known artificial sample, takes 6 hr to run on the amino-acid analyzer. Thus at the present time, chromatography is a slow and expensive process.

Attempts to speed the process and/or to cut cost generally lead to increased peak overlap (poorer spectrographic resolution). The purpose of the rubber-mask experimentation has therefore been to develop a means, by data processing, to resolve peaks in spite of heavy overlapping and to find their respective areas with great accuracy.

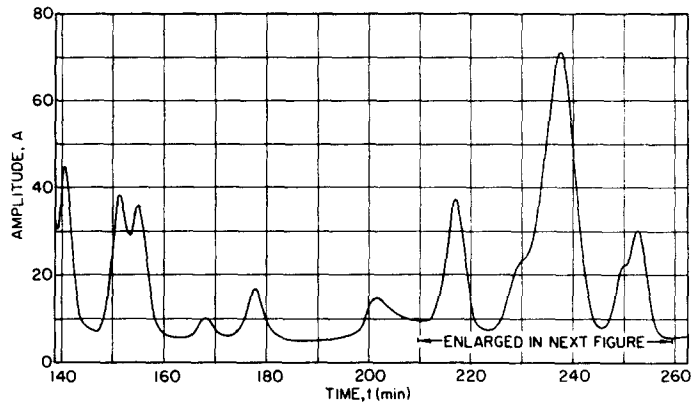

FIG. 9. Portion of chromatogram from amino acid analyzer.

In Fig. 9, a portion of a chromatogram of a typical sample is shown. Eleven peaks are present in this portion. A five-peak section of the same data is shown on an expanded scale in Fig. 10. The approach taken is to evolve a rubber mask (stretchable template) and fit it to the data. The rubber mask consists of a sum of adjustable gaussian peaks. The peaks are not fitted one at a time, but *all together* in the same process. Each peak has three parameters: position in time t_0, amplitude A, and narrowness $1/2\sigma^2$, where σ is the standard deviation. Thus the fit illustrated in Fig. 10 involves these three parameters tailored for each of the five peaks, plus an additive constant for baseline adjustment. The fit shown is very close and is typical of the results obtained with the rubber-mask

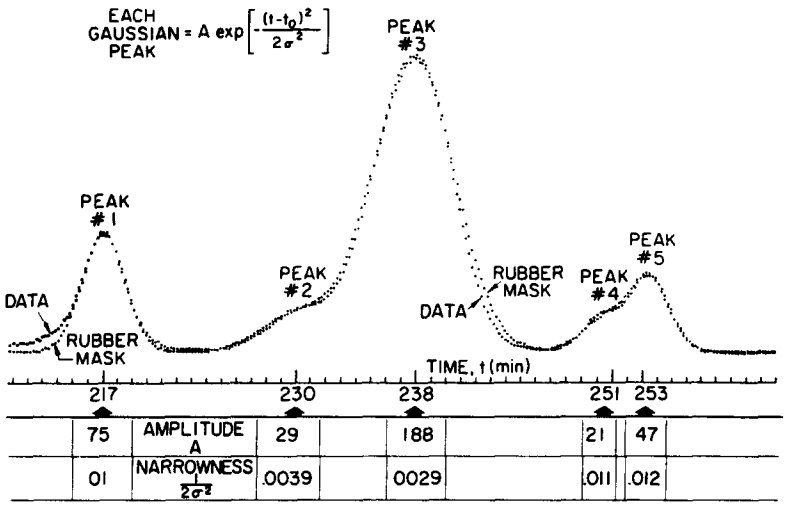

FIG. 10. Portion of chromatogram with fitted template.

process. The formula for the fitted rubber mask of Fig. 10 is

$$R = \text{constant} + 75e^{-(0.01)(t-217)^2} + 29e^{-(0.0039)(t-230)^2} + 188e^{-(0.0029)(t-238)^2} + 21e^{-(0.011)(t-251)^2} + 47e^{-(0.012)(t-253)^2}.$$

The suggestion of using a gaussian shape to represent such peaks comes from the chemical literature.[14–16] Diffusion processes take place in the chromatograph equipment, and the gaussian shape is the theoretical solution of the appropriate diffusion equation.

Current research problems involve the development of automatic fitting algorithms using steepest descent. Present methods are man/machine interactive. The problem of segmentation is being studied: (a) How many peaks should be included in each fitting process? (b) What happens when one hypothesizes a given number of peaks in a given portion of output record, whereas the actual number is different? (c) Will multiple-hypothesis testing be required, i.e. trial of various numbers of gaussian peaks? (d) How shall suitable initial parameters for the fitting process be determined? These questions are fairly typical of all the applications of rubber masks and are being studied in particular practical cases.

The chromatogram may be regarded as a string of impulses, one for each amino acid present, having corresponding time positions and amplitudes, convolved with the gaussian pulse shape by the diffusion process in the chromatograph equipment. The impulse string has thus gone through a linear filter having a two-sided gaussian impulse response. Deconvolution could be done with an inverse filter, which in this case would be the reciprocal of another gaussian shape in the frequency domain. This inverse shape goes to infinity in both directions, and must therefore be cut off by low-pass filtering. In the time domain, this introduces "ringing," causing false peaks. The net results of deconvolution are generally not good, and by no means comparable to the resolving ability of the rubber-mask method.

Illustrated by the example in this section is a problem which is common to many scientific instruments, such as gas chromatographs, mass spectrometers, air pollution

monitoring instruments, and other chemical and electronic resolving equipments. The problem is that of resolving overlapping spectral peaks. A good solution to this problem thus has wide practical applicability.

The rubber-mask technique has been used here in data smoothing, measurement, and analysis. Rubber masking can also be used in *data reduction.* For example, the entire data waveform shown in Fig. 10 could be well represented by the small number of gaussian parameters illustrated there.

4. ANALYSIS OF K-COMPLEXES IN EEG WAVEFORMS

Rubber-mask principles have been utilized in the analysis and classification of complex waveforms that occur in human electroencephalogram (EEG) recordings made during sleep. The signals are obtained from electrodes externally applied to the patient's scalp. This work is being done in collaboration with Dr. Vincent Zarcone, a psychiatrist in the Stanford University School of Medicine who is doing research on sleep and dreams, and with Dr. William Dement, director of the Sleep Research Laboratory, Stanford University.

The "K-wave" or "K-complex"[17–19] is of particular interest to sleep researchers. It is an electrical phenomenon having a characteristic shape which appears superposed upon the EEG background activity. Certain stages of non-dream sleep can be identified by measurement of the frequency of incidence of these waves. Detection of the K-wave in practice is uncertain because of the interference due to the background EEG activity. Also, timing and amplitude vary from K-wave to K-wave of the same patient. The result is that typically, two expert sleep-record readers might agree on the designation of K-waves only 60–80 per cent of the time.

In Fig. 11, the topmost EEG recordings are raw data exhibiting possible K-waves. These non-contiguous portions of a single EEG record were pre-selected by an automatic process as containing "candidate" K-waves. The pre-screening process, based on previous work done at the University of Florida,[20–22] utilizes a set of criteria such as the following: the signal should swing in the negative direction and exceed an amplitude threshold; then within a certain time interval, should swing in the positive direction and fall within a set of range of positive amplitudes; then should swing back toward zero within a certain time range. If such a criterion is met, then the EEG is considered to contain a candidate K-wave. (Note: tradition in electroencephalography is to plot negative signals upward.)

Since there appears to be no precise definition of a K-wave, it can only be defined by showing examples of K-waves judged "good." In order to establish a stereotype of a "good" K-wave, a mask for a given patient is formed by taking portions of the EEG sleep record that occur early in the morning, about 4–5 a.m., when there is generally a substantial quieting in the EEG. About five to ten good examples of K-waves are selected by an experienced investigator. These are averaged to make the mask according to the following procedure: Two K-waves are selected initially; the first is kept fixed while the second is best aligned as to baseline (dc level) and position along the time axis, and then stretched (first in amplitude, then in time, within about ± 15 per cent) to achieve best least-squares fit. After several iteration cycles, if the fit is satisfactory, the two K-waves are averaged. Then a third K-wave is taken and best-fitted to the average; it too is averaged in, and so forth until a useful stereotype is formed, as shown at the bottom of each column in Fig. 11.

We are concerned with evaluating candidate K-waves selected from the sleep record. Comparison between each candidate K-wave and the stereotype is done by summing the

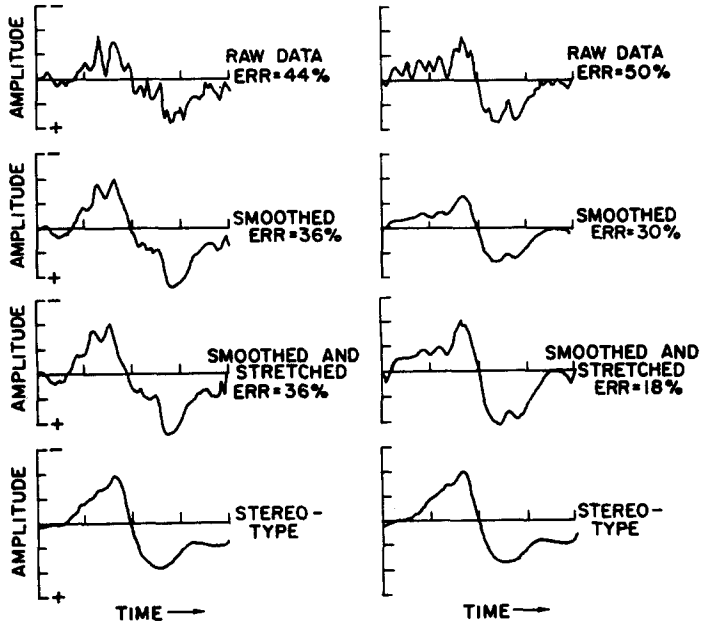

FIG. 11. Candidate K-waves from human EEG sleep recordings compared with K-wave template.

squares of sample-value differences and normalizing with respect to the sum of the squares of the sample values of the stereotype. All processing is digital. The canditate waveform is translated left–right in time and up–down in baseline level (dc level) to get a best alignment relative to the stereotype giving a minimum sum of squares of error.

In each column of Fig. 11, all of the waveforms have been compared against the stereotype when best-aligned with it, and the corresponding per cent sum-squared errors are indicated in the figure. As stated above, the topmost waveforms are two separate raw EEG events from the same patient, containing candidate waveforms. These raw data waveforms compared to the stereotype with 44 per cent and 50 per cent errors respectively. The next-to-the-top waveforms are similar to the raw-data waveforms but are filtered or smoothed versions. Smoothing is done by digital filtering using a non-recursive moving-average (tapped delay line) filter having symmetrical weights. No phase shift or phase dispersion is introduced by such a filter; only high-frequency components are altered. The raw data and the smoothed waveforms are in exact time registration. The improvement in fit from noise smoothing was significant. Reducing high-frequency noise generally cuts the sum of the squares of the errors at best fit by up to 50 per cent. In the cases shown, the smoothed data waveforms compared to the stereotype with errors of 36 per cent and 30 per cent respectively.

The next-to-the-bottom waveforms in Fig. 11 have been smoothed, best-aligned, and best-stretched (within ± 15 per cent limits in amplitude and time), and now the errors are down to 36 per cent and 18 per cent respectively. If one looks back at the raw data, the upper left-hand waveform could be rated as a 36 per cent error K-wave candidate, while the upper right-hand waveform could be rated as an 18 per cent error candidate, based on

the final best-fitted comparison. The fitting procedure allows candidate K-waves to be ranked in terms of how closely their "intrinsic shapes" match that of the stereotype.

There is considerable interest among the Stanford Sleep Research group in the use of such a ranking system. With a moderate amount of experience, this type of ranking seems to agree quite well with that obtained from skilled human scoring of the original sleep EEG record.

It should be noted that in this work, the stereotype remains fixed once it is formed. The data itself is stretched (rubberized) rather than the stereotype.

In the examples previously presented, sums of gaussian shapes (for chromatographs), or geometrically uniform artificial stereotypes (for chromosomes) were used as basic templates for the rubber mask process. In this EEG study, natural data selected by an experienced eye have been used entirely in the formation of stereotypes. The resulting stereotypes have no mathematical formula, geometric symmetry or regularity of any sort.

5. ELECTROCARDIOGRAPHIC WAVEFORM ANALYSIS

The work reported here on EKG waveform analysis has made extensive use of data obtained from Dr. J. von der Groeben of the Stanford University Medical School. From more than a thousand patients having normal heart function (as well as can be determined by clinical workup and EKG analysis), he and his associates have recorded six simultaneous EKG channels plus a seventh channel whose signal came from a strain gauge stretched across the chest to measure respiration.

The application of rubber-mask techniques to the analysis of EKG waveforms has focused on the QRS complex, defined as the main pulse of the electrocardiagram that occurs when the heart muscle "fires."

An EKG "lead" in medical terminology means an output signal of a differential amplifier whose inputs come from a pair of electrodes affixed to the patient. The use of six simultaneous anatomically affixed leads gives six different spatial projections of the complicated electrical phenomena developed during cardiac functioning.[23–25] The cardiac electrical activity is sometimes described in terms of a point electric dipole, the amplitude and direction of whose moment vector change with time during the heart beat. This description is a very rough, first order point of view, however. A more general and more adequate model consists in assuming that the electrical activity is generated by a large number of point dipoles located at different places within the heart muscle. The amplitudes and directions of these dipoles are assumed to be individual and to change with time during the beat. The actual situation is in fact more complicated, since such parameters as the size, shape, position and orientation of the heart undergo substantial mechanical changes during the heart beat. Respiration also has a marked effect on these parameters, further complicating the observed electrical phenomena.

If the heart behaved electrically like a single point dipole whose position remained stationary in space and whose amplitude and orientation changed during the beat, three linearly-independent lead signals, orthogonal or non-orthogonal, would be sufficient to precisely derive or synthesize any other projection (signal from any other lead) during the QRS. It has been found experimentally that a sixth lead can be almost perfectly synthesized by a linear combination of five other leads. Furthermore, it has been found that the QRS of a fifth lead can generally be quite closely synthesized by a linear combination of QRS's of only four other leads.

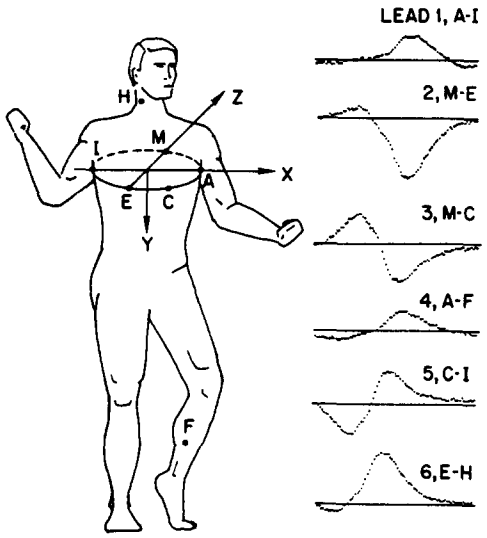

FIG. 12. Electrode placements for six-lead data.

For the EKG data used here, the placements of the six electrode leads, and typical QRS waveforms from these leads, are illustrated in Fig. 12. This lead system used by Dr. von der Groeben is similar to one proposed by FRANK.[24–26] It has been found possible to linearly combine these six leads to derive three synthetic leads which are essentially spatially orthogonal for an "average" person. Large numbers of normals, i.e. individuals having normal heartbeats, have been studied by Dr. von der Groeben using the synthesized orthogonal three-lead Frank system. In this synthetic three-space, bounds for normals during the QRS have been established. These bounds apply to magnitude in mV and to two angles in a polar coordinate system. Within a normal group for the same sex and age bracket, the QRS magnitudes in 3-space could easily vary over a 3 to 1 (or greater) range. The polar angles show a correspondingly wide range. QRS magnitude data for healthy males age 20 and younger is shown in Fig. 13.[27,28]

These findings raise certain questions. The variations from patient to patient are evidently very high, which is unfortunate. Such variations greatly complicate the problems of automatic EKG analysis. The question is, does high variability really exist from heart to heart, or is much of the evident variability in the QRS measurements caused by variations in chest shape, heart shape, location and orientation of the heart within the chest cavity, respiration, etc.? How consistent is the human heart as a pulse generator? How consistent is it from pulse to pulse, comparing pulses from the same patient, and how consistent is it from patient to patient within a normal group?

In order to analyse or classify human EKG waveforms, it is ultimately necessary to be able to compare one EKG with another. The rubber-mask idea was generalized to do this, including changes in coordinate projections along with the usual time and amplitude stretching and baseline adjustments.

As a first step, a QRS pulse from a normal patient has been compared with other QRS pulses from subsequent beats of the same patient. Beat-to-beat comparisons for a typical

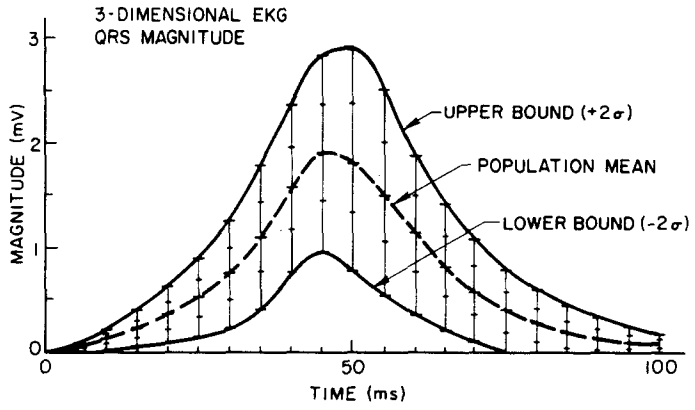

FIG. 13. Bounds of QRS magnitude for healthy males age 20 and younger observed by von der Groeben.

normal patient ("John") are shown in Fig. 14. Taking a best (in the least-squares sense) relative alignment in time and in baseline (dc level), a QRS from a *fully-inhaled* beat is compared with a QRS from a subsequent *fully-inhaled* beat in Fig. 14a. The mean-square error (m.s.e.) at best fit was 6.85 per cent for the beats shown. For most normals, this figure will vary from about 1 to 10 per cent, and will usually be of the order of a few per cent. In Fig. 14b, a QRS pulse taken at *full inspiration* is compared with a QRS at *full expiration*. Here, the per cent mean-square error is much higher; for the pulses shown the m.s.e. is 11.0 per cent. Usually, the error will run from 5 to 15 per cent, generally being about 10 per cent. It is clear from these experiments that the effects of breathing upon the shape of the QRS is highly significant, particularly when the EKG is analysed by computer rather than by "eyeball."

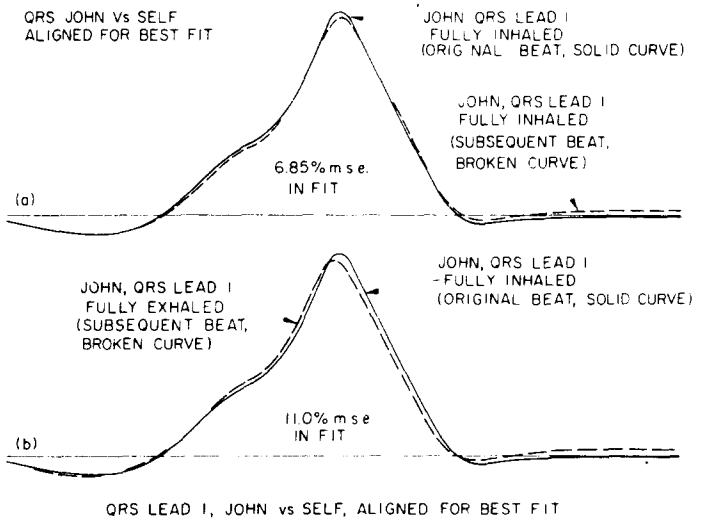

FIG. 14. Beat-to-beat comparison for John, QRS, Lead 1.

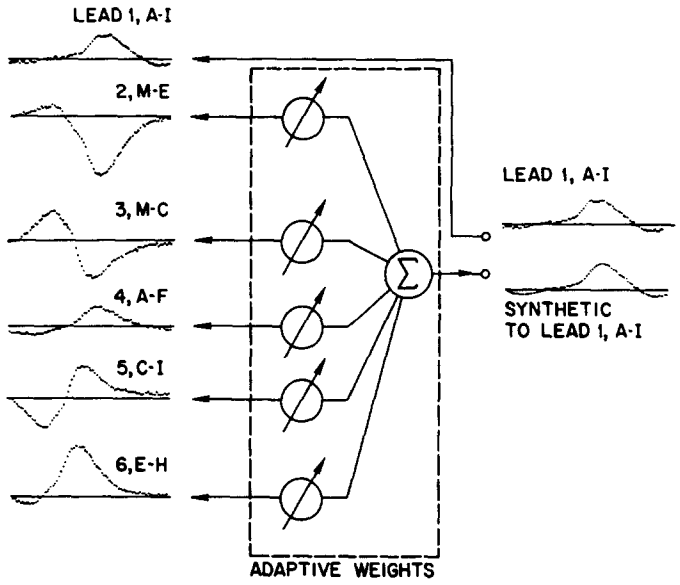

FIG. 15. Synthesis of QRS by coordinate projection.

In a recent conversation between the author and Dr. Otto H. Schmitt of the University of Minnesota, it was found that both the Stanford group and a group led by Dr. Schmitt were observing substantial beat-to-beat QRS variation due to respiration, and both groups were taking steps to remove the effects of respiration from the EKG analysis process. Dr. Schmitt has developed a simple, practical means for training the patient within a few minutes to breathe in synchronism with the R-wave (the peak of the QRS). By electronically counting R-waves, every fourth, or every fifth R-wave could be selected to light a lamp, indicating to the patient when to breathe. The patient soon develops a comfortable breathing rhythm synchronized with the EKG. Heart beats are then associated with one another in terms of time count from the R-waves which signal breathing commands. Dr. Schmitt indicated that this procedure gives excellent beat-to-beat consistency, since beats can be chosen at corresponding phases of the respiratory cycle.

The procedure described in the present paper stretches EKG waveforms in amplitude and time and by coordinate transformation in order to remove the effects of respiration. The latter evidently causes mechanical variations in the coordinate projections of the EKG leads.

A method to provide compensation for such variations is illustrated in Fig. 15. There, lead 1 is shown being synthesized as a linear combination of the remaining five leads. The weights of the linear combination (indicated by circles with arrows through them) can be adapted to achieve a best least-squares fit. This figure illustrates a general method of synthesizing desired waveforms by coordinate projection.

By adapting the synthetic projection to create a best least-squares fit between two QRS's, it appears that one is able to compensate for waveform distortions introduced not only by anatomical effects of respiration, but also by imperfect electrode placement,

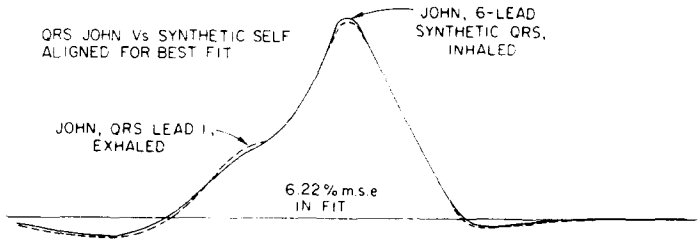

FIG. 16. Synthetic QRS John (inhaled) vs John Lead 1 (exhaled).

by variations between individuals with respect to chest shape, heart shape, location and orientation of the heart within the chest cavity, etc.

Synthetic QRS's based on linear combinations of six leads have been adapted to and compared with single-lead QRS's from the same individual. A typical result is presented in Fig. 16. For the comparison shown, best time alignment, best baseline alignment, and best weights were chosen to minimize mean-square error. Synthesizing from data of an original *fully-inhaled* beat, a fit is made to lead 1 of a subsequent *fully-exhaled* beat, resulting in 6.22 per cent mean-square error. Figure 16 compares directly with Fig. 14b, where lead 1 of the fully-inhaled beat is compared with lead 1 of the subsequent fully-exhaled beat, resulting in 11.0 per cent error. Synthetic projection has reduced the error, removing that due to respiration, and it has brought the error into the range which is typical of beat-to-beat comparison when maintaining approximately the same phase of respiration. The latter situation is represented in Fig. 14a, where the mean-square error is 6.85 per cent.

The next question to be considered is, why do EKG's look so different from person to person? Are the differences caused by intrinsic heart irregularity, or by imperfect placement of electrode leads, or by respiration, or by the impossibility of perfectly placing the electrodes in the presence of wide anatomic differences from patient to patient? To investigate these questions, we use rubber mask principles in making quantitative comparisons of EKG waveforms from patient to patient. Typical results are shown in Fig. 17.

In Fig. 17a, single beat lead-1 QRS's are taken from two patients (John and Mike, same age group) and aligned with respect to each other as best possible in time and baseline (dc level). An 88 per cent mean-square error existed. Errors of this type generally run from 50 to 150 per cent.

The m.s.e. in QRS matching between the two patients was reduced substantially by comparing a synthetic projection from six leads of one patient (John) with lead 1 of the other patient (Mike). The result is shown in Fig. 17b. The mean-square error was 32.3 per cent.

Even closer matching was obtained by incorporating a small amount of time-stretching, limiting this always to within ± 10 per cent. The time durations of the salient EKG phenomena are frequently used by cardiologists in the detection of disease. So the time base has not been stretched unduly. The effect of best time stretching along with best alignment and best projection is demonstrated in Fig. 17c. Here, the mean-square error was 9.9 per cent. It is significant to note that the mean-square error was reduced about ninefold in this example by projecting and stretching.

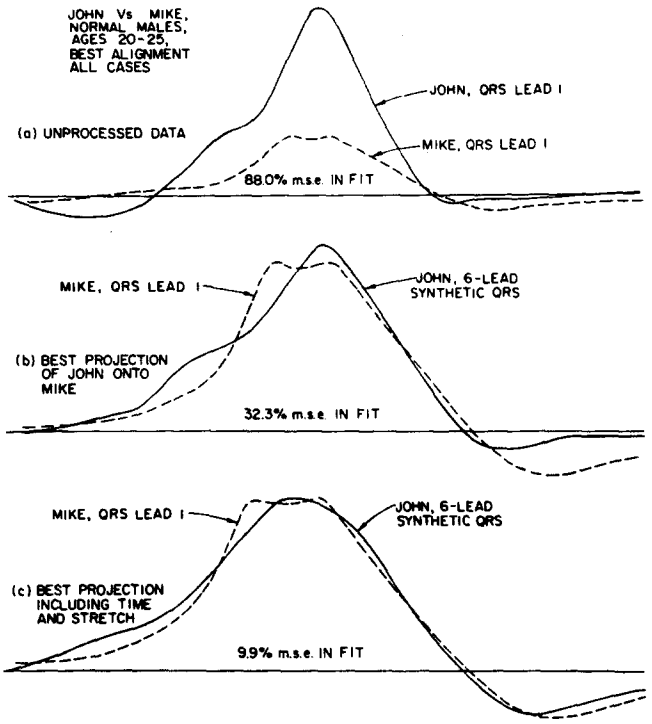

FIG. 17. Mike Lead 1 vs natural and synthetic QRS John (best projection/best projection and time stretch).

A tentative conclusion from this experiment and from many others like it is that there is far greater similarity in the *intrinsic* cardiac electrical activity than appears in comparing the EKG of one patient with that of another based on corresponding anatomical leads in accord with current clinical practice.

By the use of the rubber-mask principle as applied here to the QRS waveform, it is conceivable that a new set of $\pm 2\sigma$ bounds for normals could be derived that would be an order of magnitude tighter than those illustrated in Fig. 13.

Eliminating or reducing gross variations from QRS to QRS in the above described manner, the technique may place in evidence subtle local deviations in waveshape which may prove to be invaluable in diagnosis.

6. CONCLUSION

This paper has presented a set of examples in which the principle of rubber masks has been used in pattern measurement and analysis. Specific applications to the analysis of human chromosome images, chromatographic recordings, electrocardiogram waveforms, and electroencephalogram waveforms have been illustrated.

Previous methods of pattern analysis and recognition have in a very broad sense involved (a) template matching and (b) feature detection and classification. The rubber mask approach is based on template matching and it has many of the advantages of

template matching. It does not require the measurement of special features, the design and choice of which tend to be very problem oriented and not very general. It makes direct use of incoming and stored pattern data. The rubber mask incorporates a promising method for overcoming the difficulties associated with template matching, since flexible templates can in many cases be tolerant to the imperfections and distortions that occur in natural pattern data.

One drawback of the rubber mask approach derives from the large computational requirements of the iterative stretching and fitting process. Further work is needed to simplify the algorithms in order for these techniques to enjoy wide applicability.

Acknowledgements—I would like to thank Mrs. MABEL ROCKWELL for editing this paper and for her many useful suggestions on the organization and technical presentation. Thanks also go to Mr. SIDHARTHA MAITRA who assisted in editing. So many people have significantly contributed to this research that their assistance is acknowledged by topic:

Chromosome analysis—The problem was posed by Dr. LEONARD HAYFLICK of the Department of Medical Microbiology, Stanford University Medical School, and Mr. MICHAEL LICCARDO. The experiments were done by Mr. ROBERT MELEN, assisted by students LAWRENCE MARPLE, FRANCISCO OLIVERA and NELSON CHANG. The author is grateful to Dr. KENNETH CASTLEMAN of the Jet Propulsion Laboratory for chromosome data, and for discussions of this subject with myself and my students. Helpful discussions with Dr. MORTIMER MENDELSOHN and Mr. LEE LITTLEPAGE of the Lawrence Radiation Laboratory are gratefully acknowledged. Dr. ANN MITCHELL, Department of Pediatrics, Stanford University, has given much insight into the banding-pattern approach and its problems.

Chromatogram analysis—The problem was posed by Drs. HOWARD SUSSMAN and KLARA EFRON of the Department of Pathology, Stanford University Medical School. In addition, discussions of this work were held with Dr. DAVID KORN, Chairman of Pathology, and his thinking has had significant effect on the technical approach. The experiments were done by students DAVID NEUHOFF, DOUGLAS BLAYNEY and STANLEY TENOLD. Deconvolution analysis was done by STEVE WERNECKE.

K-wave analysis—The problem of K-wave recognition was posed by Dr. VINCENT ZARCONE of the Department of Psychiatry of the Stanford University Medical School. His help and encouragement and that of Dr. WILLIAM DEMENT were invaluable to the progress of the experiments performed by Mr. WILLIAM GIBSON.

EKG analysis—The problem was posed by the author, and the experiments were performed by students SIDHARTHA MAITRA, STEVEN ZUCKER and DAVID WEST. The assistance of Drs. JOBST VON DER GROEBEN, RICHARD CROW and CHARLES WEAVER in making EKG data available for this study and for technical discussion of computer analysis of EKG waveforms over a period of years is gratefully acknowledged.

REFERENCES

1. Matched filter issue, *IRE Trans. Information Theory* **IT-6**, 309–417 (June 1960).
2. K. STEINBUCH and U. A. W. PISKE, Learning matrices and their applications, *IEEE Trans. Electronic Computers* **EC-12**, 846–862 (1963).
3. W. H. HIGHLEYMAN, Linear decision functions, with application to pattern recognition, *Proc. IRE* **50**, 1501–1514 (1962).
4. J. S. KOFORD and G. F. GRONER, The use of an adaptive threshold element to design a linear optimal pattern classifier, *IEEE Trans. Information Theory* **IT-12**, 42–50 (1966).
5. T. M. COVER and P. E. HART, Nearest neighbor pattern classification, *IEEE Trans. Information Theory* **IT-13**, 21–27 (1967).
6. G. L. FISCHER, JR., D. K. POLLOCK, B. RADACK and M. E. STEVENS (Eds.), *Optical Character Recognition*. Spartan Books, Washington, D.C. (1962).
7. L. N. KANAL (Ed.), *Pattern Recognition*. Thompson, Washington, D.C. (1968).
8. C. N. LIU and G. L. SHELTON, JR., An experimental investigation of a mixed-font print recognition system, *IEEE Trans. Computers* **EC-15** (6), 916–925 (1966).
9. Denver Conference. A proposed standard system of nomenclature of human mitotic chromosomes, *Ann. Human Genetics* **24**, 319–324 (1960).
10. T. CASPERSSON, L. ZECH, C. JOHANSSON and E. J. MODEST, Identification of human chromosomes by DNA-binding fluorescent agents, *Chromosoma* **30**, 215–227. (1970).
11. T. CASPERSSON and L. ZECH, Chromosome identification by fluorescence. *Hospital Practice*, 51–62 (September 1972).

12. M. E. DRETS and M. W. SHAW, Specific banding patterns of human chromosomes, *Proc. Nat. Acad. Sci. U.S.A.* **68** (9), 2073–2077 (1971).
13. T. FLEISCHMANN, T. GUSTAFSSON, C. H. HAKANSSON and A. LEVAN, Computer-display of the chromosomal fluorescence pattern, *Heriditas* **68**, 325–328 (1971).
14. P. B. HAMILTON, Ion exchange chromatography of amino acids, *Anal. Chem.* **35** (13), 2055–2064 (1963).
15. H. M. GLADNEY, B. F. DOWDEN and J. D. SWALEN, Computer-assisted gas–liquid chromatography, *Anal. Chem.* **41** (7), 823–828 (1969).
16. C. D. SCOTT, D. D. CHILCOTE and W. WILSON PITT, JR., Method for resolving and measuring overlapping chromatographic peaks by use of an on-line computer with limited storage capacity, *Clin. Chem.* **16** (8), 637–642 (1970).
17. H. DAVIS, P. H. DAVIS, A. L. LOOMIS, E. N. HARVEY and G. HOBART, Electrical reactions of the human brain to auditory stimulation during sleep, *J. Neurophysiol.* **2**, 500–514 (1939).
18. L. C. JOHNSON and W. E. KARPAN, Autonomic correlates of the spontaneous K-complex, *Psychophysiology* **4** (4), 444–452 (1968).
19. J. F. SASSIN and L. C. JOHNSON, Body motility during sleep and its relation to the K-complex, *Exp. Neurol.* **22** (1), 133–144 (1968).
20. G. BREMER, Detection of the K-complex in electroencephalograms, A thesis presented to the Graduate Council of the University of Florida, University of Florida (1970).
21. G. F. BREMER, J. R. SMITH and I. KARACAN, Detection of the K-complex in electroencephalograms, *IEEE Trans. Bio-med. Engng* **17**, 314–323 (1970).
22. J. R. SMITH and I. KARACAN, EEG sleep stage scoring by an automatic hybrid system, *Electroenceph. Clin. Neurophysiol.* **31**, 231–237 (1971).
23. *Grant's Clinical Electrocardiography: The Spatial Vector Approach*, Second edition revised by J. R. BECKWITH. McGraw-Hill, New York (1970).
24. L. A. GEDDES and L. E. BAKER, *Principles of Applied Biomedical Instrumentation*. Wiley, New York (1968).
25. H. C. BURGER, *Heart and Vector: Physical Basis of Electrocardiography*. Philips Technical Library, Eindhoven, Netherlands (1968).
26. E. FRANK, An accurate, clinically practical system for spatial vectorcardiography, *Circulation* **13**, 737–749 (1956).
27. C. S. WEAVER, J. VON DER GROEBEN and H. G. GLAZE, Collecting and processing vector electrocardiograms, *Stanford Electronics Laboratories*, SU-SEL-66-122 (December 1966).
28. C. S. WEAVER, J. VON DER GROEBEN, P. E. MANTEY, C. A. COLE, JR., J. W. FITZGERALD and R. W. LAWRENCE, Digital filtering with applications to electrocardiogram processing, *IEEE Trans. Audio and Electroacoustics* **AU-16** (3), 350–391 (1968).

SELECTED READING

Chromosome image and banding pattern analysis

1. D. RUTOVITZ, Centromere finding: Some shape descriptors for small chromosome outlines, *Machine Intelligence* **5**, 435–562 (1970).
2. C. J. HILDITCH, A system of automatic chromosome analysis, *Automatic Interpretation and Classification of Images*, A. GRASSELLI (ed.) Academic, New York (1969).
3. S. STONE, L. LITTLEPAGE and B. CLEGG, Second report on the chromosome scanning program at the Lawrence Radiation Laboratory, Pattern Recognition Studies S.P.I.E. Seminar Proc., vol. 18 (1969).
4. F. RUDDLE, S. SMITH, R. LEDLEY and M. BELSON, Replication-precision study of manual and automatic chromosome analysis, *Ann. N.Y. Acad. Sci.* **157** (art 1), 400–423 (1969).
5. K. PATON, Automatic chromosome identification by the maximum likelihood method, *Ann. Human Genetics* **33**, 174–184 (1969).
6. P. NEURATH and K. ENSLEIN, Human chromosome analysis as computed from arm lengths measurements, *Cytogenetics* **8**, 337–354 (1969).
7. M. MENDELSOHN, D. HUNGERFORD, B. MAYALL, B. PERRY, T. CONWAY and J. PREWITT, Computer-oriented analysis of human chromosomes-II. *Ann. N.Y. Acad. Sci.* **157** (art 1), 376–392 (1969).
8. C. J. HILDITCH and D. RUTOVITZ, Chromosome recognition, *Ann. N.Y. Acad. Sci.* **157** (art 1), 339–364 (1969).
9. H. FREY, An interactive computer program for chromosome analysis, *Computers and Biomedical Research* **2**, 274–290 (1969).
10. J. W. BUTLER, M. K. BUTLER and B. MARCZYNSKA, Automatic analysis of 835 Mormoset Spreads, *Ann. N.Y. Acad. Sci.* **157** (art. 1), 424–437 (1969).
11. G. GALLUS, N. MONTANARO and G. MOCCACARO, A problem of pattern recognition in the automatic analysis of chromosomes; locating the centromere, *Computers and Biomedical Research* **2**, 187–197 (1968).

12. Chicago Conference: *Standardization in Human Cytogenetics*. Birth Defects: Original Article Series, II:2. The National Foundation, New York (1966).
13. P. NEURATH, B. BALOUZIAN, T. WARMS, R. SERBAGI and A. FALEK, Human chromosome analysis—an optical pattern recognition problem, *Ann. N.Y. Acad. Sci.* **128**, 1013–1028 (1966).
14. L. PENROSE *et al.*, The London Conference on the normal human karyotype, *Cytogenetics* **2**, 264–268 (1963).
15. M. A. BENDER and M. A. KASTENBAUM, Statistical analysis of the normal human karyotype, *Am. J. Human Genetics* **21** (4), 322–351 (1969).
16. C. W. GILBERT and S. MULDAL, Measurement and computer system for karyotyping human and other cells, *Nature N. B.* **230**, 203–207 (April 1971).
17. A. KLINGER, A. KOCHMAN and N. ALEXANDRIDIS, Computer analysis of chromosome patterns: Feature encoding for flexible decision making, *IEEE Trans. Computers* **C-20** (9), 1014–1022 (1971).
18. M. MENDELSOHN *et al.*, Computer oriented analysis of human chromosomes I—photometric analysis of DNA content, *Cytogenetics* **5**, 223–242 (1966).
19. S. R. PATIL, S. MERRICK and H. A. LUBS, Identification of each human chromosome with a modified giemsa strain, *Science* **173**, 821–822 (1971).
20. W. SCHNEDL, Banding patterns of human chromosomes, *Nature N.B.* **233**, 93–94 (15 September 1971).
21. T. CASPERSSON, L. ZECH, C. JOHANSSON and E. J. MODEST, Identification of human chromosomes by DNA-binding fluorescing agents, *Chromosoma* **30**, 215 (1970).
22. T. CASPERSSON, L. ZECH, and C. JOHANSSON, Analysis of the human metaphase chromosome set by aid of DNA-binding fluorescent agents, *Expl. Cell Res.* **62**, 490 (1970).
23. A. MÖLLER, H. NILSSON, T. CASPERSSON and G. LOMAKKA, Identification of human chromosome regions by aid of computerized pattern analysis, *Expl. Cell Res.* **70**, 475 (1972).
24. T. CASPERSSON, G. GAHRTON, J. LINDSTEN and L. ZECH, Identification of the Philadelphia chromosome as a number 22 by quinacrine mustard fluorescence analysis, *Expl. Cell Res.* **63**, 238 (1970).
25. T. CASPERSSON, G. LOMAKKA and L. ZECH, The 24 fluorescence patterns of the human metaphase chromosomes—distinguishing characters and variability, *Hereditas* **67**, 89 (1972).
26. T. CASPERSSON, G. LOMAKKA and A. MÖLLER, Computerized chromosome identification by aid of the quinacrine mustard fluorescence technique, *Hereditas* **67**, 103 (1971).
27. H. J. EVANS, K. E. BUCKTON and A. T. SUMNER, Cytological mapping of human chromosomes: Results obtained with quinacrine fluorescence and the acetic-saline-giemsa techniques, *Chromosoma* **35**, 310–325 (1971).
28. W. SCHNEDL, Analysis of the human karyotype using a reassociation technique, *Chromosoma* **34**, 448–454 (1971).
29. G. MANOLOV, Y. MANOLOVA and A. LEVAN, The fluorescence pattern of the human karyotype, *Hereditas* **69**, 273–286 (1971).
30. W. UNAKUL, R. T. JOHNSON, P. N. RAO and T. C. HSU, Giemsa banding of interphase HeLa chromosomes, *J. Cell Biol.* **55**, 264a (1972).
31. J. G. GALL and M. L. PARDUE, Nucleic acid hybridization in cytological preparations, *Methods in Enzymology, Nucleic Acids Part D*. L. GROSSMAN and K. MOLDAVE (Eds.) Vol. 21, pp. 470–480 (1971).
32. F. E. ARRIGHI and T. C. HSU, Localization of heterochromatin in human chromosomes, *Cytogenetics* **10**, 81–86 (1971).
33. B. DUTRILLAUX and J. LEJEUNE, *C.R. Acad. Sci., Paris* **272**, 2638–2640 (1971).
34. M. E. DRETS and M. W. SHAW, Specific banding patterns of human chromosomes, *Proc. Nat. Acad. Sci. U.S.A.* **68** (9), 2073–2077 (1971).
35. M. SEABRIGHT, A rapid banding technique for human chromosomes, *Lancet* **2**, 971–972 (1971).
36. Section of Cell Biology, M. D. Anderson Hospital and Tumor Institute, *Mammalian Chromosomes Newsl.* **13**, 21–47 (1972).

Analysis of spectrograms and chromatograms

1. D. G. LUENBERGER, Resolution of mass spectrometer data, Stanford Electronics Laboratories, Stanford, Calif., Tech. Report. SEL-64-129 (TR 6451-1) (November 1964).
2. L. R. SYNDER, A rapid approach to selecting the best experimental conditions for high-speed liquid column chromatography. Part 1, *J. Chromatog. Sci.* **10**, 200–212 (1972).

Computer analysis of EKG waveforms

1. R. HELM, An accurate lead system for spatial vectorcardiography, *Am. Heart Jl.* **53**, 415 (1957).
2. H. R. WARNER, A. F. TORONTO, L. G. VEASEY and R. STEPHENSON, A mathematical approach to medical diagnosis, application to congenital heart disease, *J.A.M.A.* 3, No. 177, 177–183 (1961).
3. C. A. STEINBERG, S. ABRAHAM and C. A. CACERES, Pattern recognition in the clinical electrocardiogram, *IRE Trans. Bio-medical Electronics* **BME-9**, 23–30 (1962).

4. L. STARK, M. OKAJIMA and G. H. WHIPPLE, Computer pattern recognition techniques; electrocardiographic diagnosis, *Commun. ACM* **5**, 527–532 (10 October 1962).
5. H. V. PIPBERGER, Use of computers in interpretation of electrocardiograms, *Circulation Res.* **11**, 555 (1962).
6. T. Y. YOUNG and W. H. HUGGINS, Computer analysis of electrocardiograms using a linear regression technique, *IEEE Trans. Bio-medical Engineering* **BME-11**, 60–67 (July 1964).
7. D. F. SPECHT, Vectorcardiographic diagnosis using the polynominal discriminant method of pattern recognition, *IEEE Trans. Bio-medical Engineering* **BME-14** (2), 90–95 (1967).
8. J. P. BROWN, D. B. FRANCIS, T. W. CALVERT and R. L. LONGINI, Compensating the VCG for anatomic variations of individuals, Proc. Annual Conf. on Engineering in Biology and Medicine, Boston, Mass. (November 1967).
9. J. P. BROWN, T. W. CALVERT, R. L. LONGINI and E. W. HECKERT, Normalizing the VCG to facilitate diagnosis, Proc. Annual Conf. on Engineering in Biology and Medicine, Houston, Texas (1968).
10. A. A. LANGER, R. L. LONGINI and E. W. HECKET, Body compensator system for VCG's, Proc. 8th Int. Conf. on Medical and Biological Engineering, Chicago, Illinois (1969).
11. R. GAMBOA, J. D. KLINGEMAN and H. V. PIPBERGER, Computer diagnosis of biventricular hypertrophy from orthogonal electrocardiograms, *Circulation* **39**, 72–82 (January 1969).
12. D. B. GESELOWITZ and O. H. SCHMITT, Electrocardiography, *Biomedical Engineering*, H. P. SCHWANN (ed.) McGraw-Hill, New York (1969).
13. J. VON DER GROEBEN, J. G. TOOLE and C. S. WEAVER, Vectorcardiographic analysis with the aid of a small digital computer, *Actuelle Probleme der Vektorkardiographie*, R. WENGER (ed.) Georg Thieme, Stuttgart (1968).
14. W. P. HOLSINGER, K. M. KEMPUER and M. H. MILLER, A QRS preprocessor based on digital differentiation, *IEEE Trans. Bio-medical Engineering* **BME-18** (3), 212–217 (May 1971).
15. D. B. GESELOWITZ, Use of the multipole expansion to extract significant features of the surface electrocardiogram, *IEEE Trans. Computers* **C-20** (9), 1086–1089 (September 1971).
16. R. PLONSEY, Capability and limitations of electrocardiography and magnetocardiography, *IEEE Trans. Bio-medical Engineering* **BME-19** (3), 239–244 (May 1972).

Other work with flexible templates and parametrized descriptions of patterns

1. R. G. CASEY and G. PURDY, Moment normalization of handprinted characters, *IBM Research*, Yorktown Heights, New York: RC 2666 (14 October 1969).
2. H. J. BREMERMANN, Pattern recognition by means of deformable prototypes, a talk presented at the 1971 Workshop on Pattern Recognition, Anaheim, Calif., October 27, 1971; abstracted on p. 547, *IEEE Trans. Systems, Man and Cybernetics* **SMC-2** (4), (September 1972).
3. C. T. ZAHN and R. Z. ROSKIES, Fourier descriptors for plane closed curves, *IEEE Trans. Computers* **C-21**, 269–281 (1972).
4. T. CASPERSSON and L. ZECH, Chromosome identification by fluorescence, *Hospital Practice* **7** (9), 51–62 (1972).

General bio-medical pattern recognition

1. R. S. LEDLEY and L. S. ROTOLO, Application of pattern recognition to biomedical problems, *Automatic Interpretation and Classification of Images*, A. GRASSELLI (ed.), pp. 323–362. Academic Press, New York (1969).
2. C. J. HILDITCH, A system of automatic chromosome analysis, *Ibid* 363–390, (1969).
3. M. PFEILER, Image transmission and image processing in radiology, *Ibid* 399–416 (1969).
4. R. S. LEDLEY, Automatic pattern recognition for clinical medicine, *Proc. IEEE* **57** (11), 2017–2035 (1969).
5. E. E. GOSE, Introduction to biological and mechanical pattern recognition, *Methodologies of Pattern Recognition*, S. WATANABE (ed.) pp. 203–253. Academic Press, New York (1969).
6. E. E. GOSE, J. W. BACUS and L. V. ACKERMAN, A comparison of some computer-measured and human-measured pattern recognition properties, *J. Cybernetics* **1** (4), 68–74 (1971).
7. J. W. BACUS and E. E. GOSE, Leukocyte pattern recognition, *IEEE Trans. Systems, Man, and Cybernetics* **SMC-2** (4), 513–525 (1972).
8. R. LEDLEY, F. RUDDLE, J. WILSON, M. BELSON and J. ALBARRAN, The case of touching and overlapping chromosomes, *Pictorial Pattern Recognition*, G. CHENG *et al.* (eds.) pp. 87–97. Thompson (1968).
9. R. LEDLEY, Automatic pattern recognition for clinical medicine, *Proc. IEEE* **57**, 2017–2035 (1969).
10. K. PATON, An automatic method for finding metaphase spreads, *Pictorial Pattern Recognition*, G. CHENG *et al.* (eds.) pp. 135–146. Thompson (1968).
11. R. LEDLEY, M. LEGATOR and J. WILSON, Automatic determination of mitotic index, *Pictorial Pattern Recognition*, G. CHENG *et al.* (eds.) pp. 99–103. Thompson (1968).

12. J. W. BUTLER, M. K. BUTLER and A. STROUD, Automatic classification of chromosomes—II, and Automatic classification of chromosomes—III, *Data Acquisition and Processing in Biology and Medicine*, K. ENSLEIN (ed.), pp. 45–57 and pp. 21–37. Pergamon, Oxford (1965 and 1968).
13. R. LEDLEY, FIDAC: Film input to digital automatic computer and associated syntax directed pattern recognition programming system, *Optical and Electro-Optical Information Processing*, J. TIPPETT *et al.* (eds.) Chapter 33, pp. 591–612. MIT Press (1965).
14. R. LEDLEY, High speed automatic analysis of biomedical pictures, *Science* **146**, 216–223 (9 October 1964).
15. K. ENSLEIN and P. W. NEURATH, Augmented stepwise discriminent analysis applied to two classification problems in the biomedical field, *Computers and Biomedical Research* **2**, 568–581 (1969).
16. D. RUTOVITZ, Pattern recognition, *Royal Statistical Society* **12a**, 504–530, series A (1966).
17. R. STEFANELLI and A. ROSENFELD, Some parallel thinning algorithms for digital pictures, *J. ACM* **18** (2) 255–264 (1971).
18. J. HILDITCH and D. RUTOVITZ, Chromosome recognition, *Ann. N.Y. Acad. Sci.* **157**, 339–364 (1969).
19. M. INGRAM, P. E. NORGREN and K. PRESTON, JR. Automatic differentiation of white blood cells, *Image Processing in Biological Sciences*, D. M. RAMSEY (ed.) Univ. Calif. Press, Berkeley, Calif. (1968).
20. M. INGRAM and K. PRESTON, JR., Automatic analysis of blood cells, *Scient. Am.* **223**, 72–82 (1970).
21. M. L. MENDELSOHN, B. H. MAYALL, J. M. S. PREWITT, R. C. BOSTROM and W. G. HOLCOMB, Digital transformations and computer analysis of microscopic images, *Advances in Optical and Electron Microscopy*, V. E. COSLETT (ed.) pp. 77–150. Academic, New York (1968).
22. J. M. S. PREWITT and M. L. MENDELSOHN, A general approach to image analysis by parameter extraction, Proc. Computers in Radiology, Chicago (1966).
23. The analysis of cell images, *Ann. N.Y. Acad. Sci.* **128**, 1035–1053 (1966).
24. T. GOLAB, R. S. LEDLEY and L. S. ROTOLO, FIDAC—Film input to digital computer, *Pattern Recognition* **3**, 123 (1971).